2015-01-01

AC-Susceptibility Investigations of Superspin Blocking and Freezing in Interacting Magnetic Nanoparticle Ensembles

Joshua Logan Morris
University of Texas at El Paso, jlmorris2@miners.utep.edu

AC-SUSCEPTIBILITY INVESTIGATIONS OF SUPERSPIN BLOCKING AND FREEZING IN INTERACTING MAGNETIC NANOPARTICLE ENSEMBLES

JOSHUA LOGAN MORRIS

Department of Physics

APPROVED:

Cristian E. Botez, Ph.D., Chair

Chunqiang Li, Ph.D.

Russell Chianelli, Ph.D.

Charles Ambler, Ph.D.
Dean of the Graduate School

Dedication

I dedicate this to all my friends and family as they've been the solid foundation upon which I've tried to build myself into the best person I could be.

If I have seen further it is by standing on the shoulders of giants – Sir Isaac Newton

AC-SUSCEPTIBILITY INVESTIGATIONS OF SUPERSPIN BLOCKING AND FREEZING IN INTERACTING MAGNETIC NANOPARTICLE ENSEMBLES

by

JOSHUA LOGAN MORRIS, B.S

THESIS

Presented to the Faculty of the Graduate School of

The University of Texas at El Paso

in Partial Fulfillment

of the Requirements

for the Degree of

MASTER OF SCIENCE

Department of Physics

THE UNIVERSITY OF TEXAS AT EL PASO

August 2015

Acknowledgements

I would like to first acknowledge support from the National Institutes of Health under the Maximizing Access to Research Careers (MARC) program, Award No. 2T34GM008048, as they supported my initial work into magnetism and supported my work as I began this project. The completion of this project would not have been possible without the support of the Donors of the American Chemical Society Petroleum Research Fund, Awards No. 45854-GB10 and 52216-UR10 with further support from the U.S. Department of Defense Army Research Office under Award No. 64705CHREP.

Next I would like to acknowledge Dr. Cristian E. Botez for his mentorship and guidance. While I learned a great deal about the research process from him throughout my four-plus years working with him, it's the snippets of wisdom that I learned outside of the lab that will have a powerful and lasting effect on me as a scientist and person.

Dr. Keith Pannell also deserves more thanks than can be expressed here for believing in me and funding me as a young scientist. Without his experience, wit, and down-to-business attitude helping to positively influence my development, I would not be where I am today.

Lastly I would like to acknowledge my parents and Allissa for their constant support and for keeping me grounded since there's so much more to life than what goes on in the classroom and research lab. You all mean more to me than words can describe.

Abstract

We have investigated the effect of dipolar interactions on the superspin blocking and freezing of 10 nm average size Fe_3O_4 magnetic nanoparticle ensembles. Our dynamic susceptibility data reveals a two-regime behavior of the blocking temperature, T_B, upon diluting a Fe_3O_4/hexane magnetic nanoparticle fluid. As the nanoparticle volume ratio, Φ, is reduced from an as-prepared reference $\Phi = 1$ to $\Phi = 1/96$, the blocking temperature decreases from 46.1 K to 34.2 K, but higher values reenter upon further diluting the magnetic fluid to $\Phi = 1/384$ (where $T_B = 42.5$ K). We show that cooling below T_B within the higher concentration range ($\Phi > 1/48$) leads to the collective freezing of the superspins in a spin-glass-like fashion, whereas individual superspin blocking occurs in the presence of weaker dipolar interactions ($\Phi < 1/96$). The unexpected increase of the blocking temperature with the decrease of the interparticle interactions observed at low nanoparticle concentrations is well described by the Mørup-Tronc (MT) model.

Table of Contents

List of Figures

Chapter 1: Magnetic Phenomena

Magnetic nanoparticle ensembles have been the subject of much research in the last century. The current and potential applications in biomedicine and in emerging technologies such as the development of high density magnetic storage media have garnered much of the recent attention on these systems. Key to the functionality and applicability are the microstructure and mechanisms that make them exhibit unique properties and behave differently from their bulk counterparts. Each nanoparticle below a critical size becomes a single magnetic domain, as opposed to the multiple domain bulk material. A complete description of how single magnetic domain systems behave between the regions of a non-interacting system and strongly interacting system is not yet fully established. While non-interacting systems behave as superparamagnets and highly dense systems behave as superspin-glasses, what phenomena occur between these extremes remains a topic of continuing research and discussion.

1.1 Application of Magnetic Domains

Over the past two decades, much work has been devoted to investigations of these single domain magnetic nanoparticles, as these systems have current and potential applications in emerging technologies in important areas such as next-generation high-density magnetic recording [1], magnetic refrigeration [2], and biomedicine (magnetic nanoparticle hyperthermia, e.g.) [3-5]. For many of these applications, understanding the effect of the interparticle dipolar interactions on the macroscopic magnetic behavior of the ensemble is of critical importance. For example, strong dipolar interactions have been reported to lead to collective phenomena [6-13], and this would clearly affect the functionality of high-density magnetic recording devices where each superspin is used as a recording bit that needs to be able to individually respond during the recording process. Elucidating the effects of interparticle dipolar interactions on nanoparticle

response behavior is then of paramount importance in advancing the quantitative description of these effects.

1.2 Models of Interacting Systems

Due to the similarity of their basic ac-susceptibility signature — a peak in the χ" vs. T dependence — distinguishing between superparamagnetic blocking [14,15] and collective spin-glass-like freezing (of either surface spins [16,17] or the superspins [18,19]) is often not straightforward. Models based on the differing strength of interparticle interaction allow for fits to the ac-susceptibility data to determine the type of nanoparticle behavior is most prevalent in nanoparticle ensembles.

1.2.1 Non-Interacting Systems

For an ensemble of *non-interacting* (ideal) magnetic nanoparticles, the individual superspin dynamics are explained by the Néel-Brown activation law:

$$\tau(T) = \tau_0 \exp\left(\frac{E_B}{k_B T}\right) \qquad (1)$$

which describes the temperature dependence of the system's relaxation time τ, (the time it takes each nanoparticle's magnetic moment to flip across an anisotropy energy barrier E_B). Here, τ_0 is the inverse attempt frequency, k_B is Boltzmann's constant, and T is the temperature. The energy barrier to magnetization reversal has been empirically defined as $E_B(\theta) = KV \sin^2\theta$, where K is the magnetic anisotropy constant, V is the particle volume, and θ is the angle between the magnetization vector and the direction of an easy magnetization axis; for uniaxial particles the energy becomes $E_B = KV$. If one carries out an ac-magnetic susceptibility measurement on such

a system, the observation time τ_{obs} is proportional to the inverse of the measurement frequency, $\tau_{obs} = 1/2\pi f_{obs}$. If dc-magnetization measurements are performed, τ_{obs} is typically considered to be on the order of ~1s. The temperature at which the observation time equals the ensemble's relaxation time (i.e. $\tau_{obs} = \tau$) is then defined as the blocking temperature T_B. For a non-interacting nanoparticle system T_B is expressed as:

$$T_B = \frac{E_B}{k_B \ln(\tau/\tau_0)} \qquad (2)$$

Above T_B, the nanoparticles' magnetic moments fluctuate rapidly, and the ensemble behaves similarly to a paramagnet. Below T_B, however, the thermal energy is insufficient to exceed E_B, and the superspins are "blocked" along an easy magnetization axis. Due to this blocking behavior, the (super)paramagnetic magnetization and associated magnetic susceptibility reach a maximum at T_B and decrease upon further cooling [20,21]. In practice, however, interactions between the magnetic nanoparticles are always present, and, depending on their strength, can have different effects on the relaxation and blocking of the superspins. This phenomenon in turn gives rise to the previously mentioned collective spin-glass-like behavior for sufficiently strong interactions.

1.2.2 Strongly Interacting Systems

With increasing particle concentration, the effects of *strong* dipolar interactions eventually lead to qualitatively different magnetic behaviors, where, upon cooling below a critical temperature, the superspins freeze in a spin-like-glass fashion rather that individually blocking [22-24]. This has been confirmed by several recent studies and explained on the basis of the conventional dynamic scaling theory which holds that the relaxation time τ of a system

diverges as a power law with the correlation length ξ, such that $\tau=\tau_0\xi^z$. Here τ_0 is the characteristic time related to the attempt frequency, $\tau_o=1/2\pi f_o$, and z is a dynamic scaling exponent. In addition, according to the static scaling hypothesis, a temperature-dependent correlation length is then defined as $\xi=[(T/T_g)-1]^{\nu}$, where T_g is the critical spin-glass freezing temperature and ν is a critical exponent. Eventually, one finds:

$$\tau = \tau_0 \left[\frac{T}{T_g} - 1 \right]^{-z\nu} \qquad (3).$$

where τ is related to the observation frequency f by $\tau=1/2\pi f$. In such nanoparticle ensembles (where superspin freezing due to strong interparticle interactions occurs upon cooling) the blocking temperature has been found to increase with the increase of the interaction strength, which, in most experiments, is controlled by varying the interparticle distance.

It is important to note that T_B and T_g are fundamentally different parameters related to the measurement time of the ensemble (T_B) and a characteristic temperature (T_g) below which spin-glass freezing effects can be observed.

1.3 Quantifying Behaviors of Interacting Systems

1.3.1 Weakly Interacting Systems

For *weaker* dipolar interactions, magnetic nanoparticle ensembles exhibit the same individual superspin blocking behavior as their ideal, non-interacting counterparts, but calculating the superparamagnetic relaxation times in real systems even for weakly interacting particles is an extremely complex task, and only models based on approximations are available.

One such model was proposed by Shtrikman and Wohlfarth (SW) and centers on a Vogel-Fulcher activation law:

$$\tau(T) = \tau_0 \exp\left(\frac{E_B}{k_B(T - T_0)}\right) \qquad (4)$$

where T_0 describes the strength of the interactions [25]. Another model was proposed by Dormann, Bessais and Fiorani (DBF) who calculated the interaction energy E_{int} and added it to the energy barrier in the expression of the magnetic relaxation time:

$$\tau(T) = \tau_0 \exp\left(\frac{E_{\text{int}} + E_B}{k_B T}\right) \qquad (5)$$

Both the SW and the DBF models predict an increase of the relaxation time, τ (and corresponding blocking temperature T_B) with the increase of the interparticle interaction strength.

1.3.1 The Mørup-Tronc Model for Increasing Interaction Strength

A third model was proposed by Mørup and Tronc (MT) for very weak interactions, i.e. $\mu\langle B_i\rangle/2KV << 1$, where μ is the magnetic moment of the nanoparticle and B_i is the average dipolar field at particle *i* [26]. Interestingly, the MT model predicts that both τ and T_B *decrease* as the strength of the dipolar interactions increases. The blocking temperature is given by:

$$T_B = \frac{KV}{k_B C}\left[1 - h_{av}^2\left(\frac{4}{3}C - 1\right)\right] \qquad (6)$$

where $h_{av}^2 = \mu^2\langle B_i^2\rangle/(2KV)^2$ and C is a constant related to the measurement/observation time by $C = \ln(\tau_{obs}/\tau_0)$. Using the expression of the average dipolar field at particle i in an ensemble of magnetic nanoparticles [26], one finds that the reduction of T_B occurs as h_{av} strengthens upon the decrease of the interparticle distance, according to:

$$h_{av}^2 = \frac{\mu_0^2 M^4 \varepsilon^{-6}}{1152K^2}\sum_j a_{ij}^{-6} \qquad (7)$$

Here, M is the saturation magnetization, ε is a measure of the interparticle distance that depends on the nanoparticle volume ratio according to the relationship $d_{ij} = a_{ij}\varepsilon D$ (where D is the average diameter of the nanoparticles); the summation over all particles, Σa_{ij}^{-6} , is independent of both the particle size and concentration and ranges is of the order of 10-20.

The volume ratio, Φ, is defined as the particle volume over the total volume. This leads to the relationship $\Phi^{1/3} \propto D/d$ where d is defined above. This leads to the relationship between ε and Φ:

$$\varepsilon = \frac{d_{ij}}{D} = \Phi^{-1/3} \Rightarrow \quad \varepsilon^{-6} \propto \Phi^2 \qquad (8)$$

In conjunction with Eqn. (6), the blocking temperature is then predicted to *decrease* with an increasing nanoparticle volume ratio.

1.3.2 Application of the MT Model to Nanoparticle Data

To date, most experimental studies based on dc-magnetization and ac-susceptibility methods show an increase of the blocking temperature with the strength of the interactions, in accordance with the SW and DBF models. However, there is one Mössbauer spectroscopy study carried out on two samples of different interparticle distances that confirms the MT prediction [27]. Recent Monte Carlo calculations predicted a non-monotonic behavior of the blocking temperature in Fe_2O_3 nanoparticle ensembles that includes two regimes separated by a critical concentration [28]. In addition, there are significant observed differences between the magnitude of the effect of dipolar interactions on T_B reported by different studies [10, 29-32]. Consequently, more investigation is needed to further clarify how the average distance between magnetic nanoparticles (and the corresponding interparticle dipolar interactions) influence the superspin dynamics and blocking behavior of these systems.

Here, we report ac magnetic susceptibility measurements carried out on Fe_3O_4/hexane magnetic fluids of nine different nanoparticle volume ratios, Φ, ranging from $\Phi = 1$ (an as-prepared reference) to $\Phi = 1/384$. For each Φ, we recorded the temperature dependence of the out-of-phase susceptibility χ" within the 5 K – 80 K range at five different frequencies between 100 and 10000 Hz. Our data reveal two distinct regimes in terms of the relaxation time τ / blocking temperature T_B behavior upon dilution. First, we find that T_B monotonically decreases from 46.1 K to 34.2 K as Φ is reduced from 1 to 1/96. Most of this range is associated with strong inter-particle interactions, where the ensemble of superspins freezes collectively in a spin-glass-like-fashion below a temperature threshold. Interestingly, further diluting the system ($\Phi <$ 1/96) leads to the opposite effect, where T_B increases with the decrease of Φ, reaching $T_B = 42.5$

K at $\Phi = 1/384$. We find this behavior of T_B in the weak-dipolar-interaction-regime to be excellently described by the MT model.

Chapter 2: Experimental Methods

2.1 Sample Preparation

All measurements were collected on ensembles of Fe_3O_4 nanoparticles immersed in hexane, at temperatures below the freezing point of the carrier fluid. The crystal structure and purity of the Fe_3O_4 nanopowder were confirmed by laboratory x-ray diffraction analysis carried out on a Siemens D5000 diffractometer (λ = 1.5406 Å). The sample was loaded in a flat-plate holder and diffraction patterns were collected in the reflectivity geometry for d-spacing values between 1.5 Å and 3.5 Å (equivalent to the 20˚ - 60˚ detector angle 2θ range). The data collection time for each diffraction pattern was approximately 60 min. The process was repeated several times to ensure the reproducibility of the results. No significant difference was observed between the experimental runs. These data sets were then analyzed using a full-profile (Le Bial) fit [33] to the data. Using the full-width at half-maximum of the diffraction patter, the average size of the nanoparticle ensembles can then be calculated from Scherrer analysis ([22]) where the average diameter is given by:

$$\langle D \rangle = \frac{K\lambda}{\beta_{FWHM} \cos\theta_{peak}}$$

We performed the analysis with Scherrer's constant set to unity, $K = 1$, and θ_{peak} set to the angle of the peak reflection as determined from the Le Bial analysis. The average particle size was then calculated to be $\langle D \rangle$ = 10 nm.

The initial ferrofluid sample (nanoparticle reference volume ratio Φ = 1) was subsequently diluted to Φ values of 1/3, 1/12, 1/24, 1/48, 1/96, 1/192, 1/240, 1/384. Each subsequent measurement was then carried out on the same initial sample following identical dilution protocols.

2.2 Measurement Techniques

All magnetization measurements were then carried out on a Quantum Design® Physical Property Measurement System (PPMS). Approximately 5 mL of the ferrofluid was injected into a polycarbonate capsule for loading in the sample rod. The sample was then lowered into the cryostat of the PPMS. A visualization of the inter-chamber configuration of the PPMS is presented at the end of the chapter for reference.

Dc-magnetization measurements are conducted by lowering the sample into the coil assembly and applying a direct current. The constant magnetic field produced as a result of the dc current is then used in correlation with perturbations in the magnetic induction due to the interaction of the field ($\mathbf{M} \propto \chi_m \mathbf{B}$) and the nanoparticles. The induced voltage is then measured and the magnetization is then recorded as a function of temperature. Measurements are typically conducted at a low |H| field (< 100 Oe).

In zero-field-cooled measurements, the sample is cooled from its initial temperature to the starting measurement temperature. The PPMS motor system then raises and lowers the coil assembly to induce the current that is then measured. The magnetization is recorded in the presence of the constant field with increasing temperature. For field-cooled measurements, the sample is cooled under the constant field and then magnetization is measured using an identical protocol.

Ac-susceptibility measurements are conducted by again lowering the sample into the coil assembly and cooling. A high-frequency ac current is then applied as both the coil assembly and sample probe remain stationary. The high-frequency alternating magnetic field in turn causes a current response from the nanoparticle assembly. The delay in the nanoparticle response

corresponds to a phase shift composed of two components. The in-phase (real) and out-of-phase (imaginary) components are measured as a function of temperature for a constant frequency. These measurements are typically carried out a low field amplitude $|H| \leq 100$ Oe.

Dc-magnetization measurements were first performed on the undiluted sample. A zero-field-cooled field-cooled (FC-ZFC) dc-magnetization measurement protocol was performed and data were recorded upon heating the magnetic nanoparticle system from 5 to 140 K in a constant 50 Oe external magnetic field.

Frequency-resolved ac-susceptibility measurements were then performed on each sample from data $\Phi = 1$ to $\Phi = 1/384$ upon heating from 5 to 80 K. The amplitude of the oscillating magnetic field was 5 Oe and the frequencies used were 100 Hz, 300 Hz, 1000 Hz, 3000 Hz, and 10000 Hz. Identical measurement protocols were repeated for each dilution and each set of measurements were performed on the sample encased in a clean polycarbonate capsule.

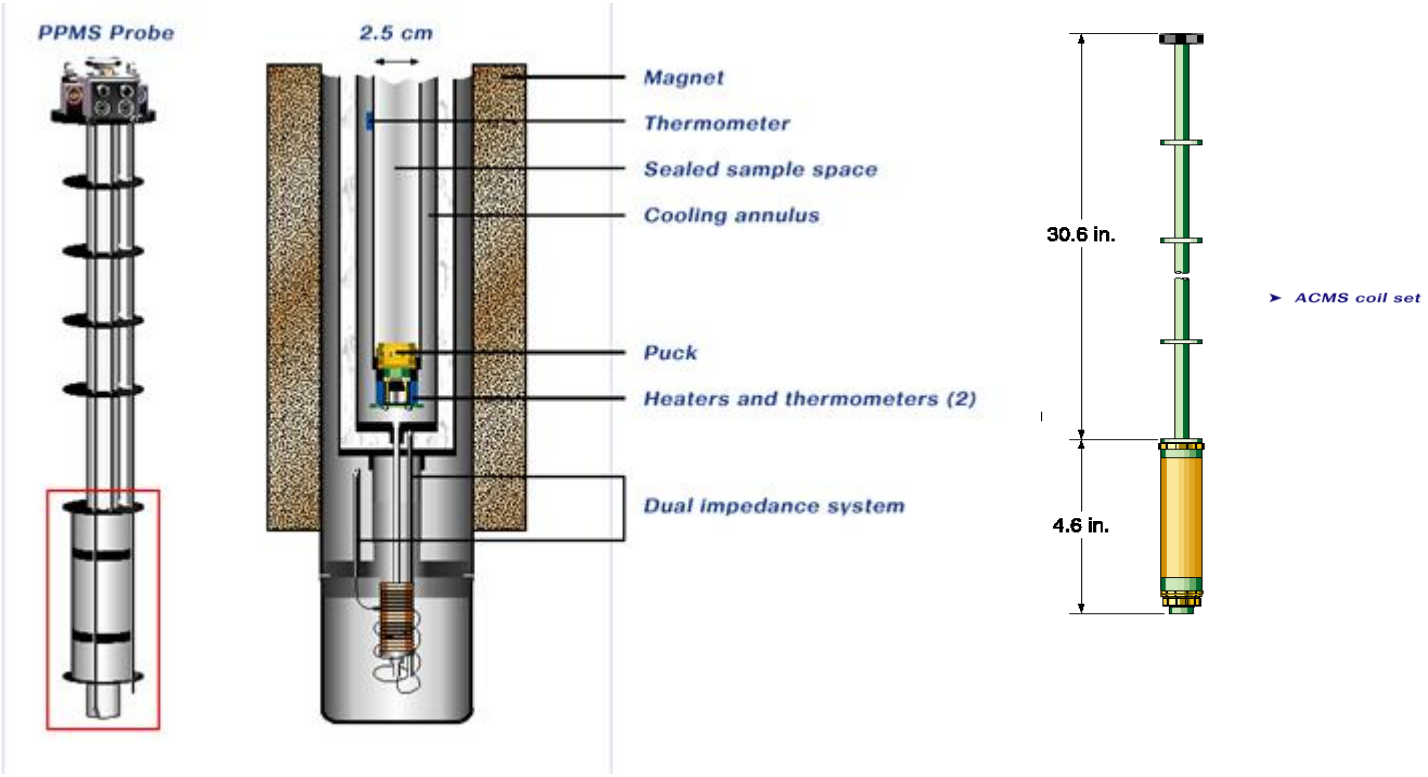

Chapter 3: Results and Discussions

3.1 Observed Spin-Glass and Superparamagnetic Behavior

Figure 1 shows the temperature dependence of the dc-magnetization, M vs. T, recorded on the (Φ = 1/3) Fe_3O_4 nanoparticle ensemble upon heating from 4 K to 140 K under an externally applied magnetic field of 50 Oe. The solid symbols represent the zero-field-cooled (ZFC) M vs. T curve measured after cooling down from room temperature in the absence of any external field, whereas the empty symbols show its field-cooled (FC) M vs. T counterpart collected after cooling in the presence of the 50 Oe field. The FC and ZFC magnetization branches overlap in the superparamagnetic regime, where M decreases with increasing T as a Langevin function [34], but split below a critical temperature that marks the onset of irreversibility. While such a behavior is most often regarded as being due to individual superspin blocking [35], there are several other phenomena that have this signature [36-38]. Among them is the collective freezing of the superspins in a spin-glass-like fashion that occurs in magnetic nanoparticle ensembles where dipolar interparticle interactions are strong [39]. To clarify the nature of the microscopic dynamics that leads to the ZFC-FC behavior shown in Figure 1, we carried out frequency resolved ac-susceptibility measurements that can distinguish between individual superspin blocking and collective superspin freezing. These results are shown Figure 2 (a). Data were collected on the same (Φ = 1/3) Fe_3O_4 nanoparticle ensemble by measuring the temperature dependence of the out-of-phase component of the ac-susceptibility χ" within the 4 K-80 K range at five different frequencies: 10 Hz, 100 Hz, 1000 Hz, 3000 Hz, and 10000 Hz. At all frequencies, the solid lines are best fits to polynomial functions that allow the temperatures at

which the χ" vs. T curves peak to be determined. Expectedly, the peaks shift toward higher temperatures as the measurement frequency is increased. This is shown by the solid symbols in Figure 2 (b), where the ac-susceptibility peak temperature is presented as a function of the observation time τ (which is related to the measurement frequency by $\tau=1/2\pi f$). The observed behavior is well described by the dynamic scaling law commonly used to characterize canonic spin glasses. Indeed, the solid line in Figure 2 (b) is a best fit of Eq. (3) to the τ vs. T data; the fit yields a freezing temperature T_g = 38.5 K, a critical exponent $z\nu$=8.45 and time constant $\tau=6.09\times10^{-7}$ s. It is important to mention that attempts to fit the data to a Vogel-Fulcher law (Eqn. (4)) have also been successful, but yielded an unphysically large interaction parameter T_0 = 25 K.

We then collected frequency-resolved ac-susceptibility data - like the ones presented in Figure 2 (a) - and carried out similar analyses of the critical temperature shift with the observation time for samples of other nanoparticle volume ratio values: Φ = 1, 1/12, 1/24, 1/48, 1/96, 1/192, 1/240, 1/384. We found that the dynamic scaling law associated with collective superspin freezing describes the cooling-induced dynamic magnetic behavior of the samples with large Φ values, ($1/48 < \Phi < 1$), whereas the superspins in the more diluted samples ($1/384 < \Phi < 1/96$) block individually upon cooling and their dynamic behavior is described by a Vogel-Fulcher type activation law. This is not unexpected, as large nanoparticle volume ratios (i.e. short interparticle distances) result in strong interparticle dipolar interactions that have been previously observed to lead to superspin glass freezing [22-24,39].

Figure 3 (a) shows the temperature dependence of the imaginary ac susceptibility measured at a frequency of 10,000 Hz between 20 K and 60 K on Fe_3O_4 magnetic nanoparticle ensembles of volume ratios: Φ = 1, 1/3, 1/12, 1/24, 1/48, 1/96, 1/192, 1/240, and 1/384. We observe that the

χ" vs. T peak temperatures T_B shift towards lower values with the decrease of the nanoparticle volume ratio (thus with the weakening of the interparticle interactions) for Φ values between 1 and 1/48. As indicated above, nanoparticle ensembles within this Φ range undergo transitions from superparamagnetic to a superspin glass state upon cooling below T_B.

3.2 Reentrant Increase in T_B

Interestingly, a very different behavior is observed in weakly interacting samples obtained upon further dilution. Indeed, for nanoparticle ensembles with Φ values between 1/96 and 1/348, the ac-susceptibility peak temperature exhibits a reentrant *increase* with the decrease of Φ (i.e. upon the decrease of the interparticle interactions). This behavior has only been reported once by Mørup and Tronc, who studied the effect of the interparticle interactions on the dynamic relaxation behavior of γ-Fe_2O_3 nanoparticle ensembles [20]. Using Mossbauer spectroscopy, they found that the relaxation times decrease with decreasing particle interactions (or, equivalently, the blocking temperature increases with the decrease of interparticle interactions); Mørup and Tronc proposed a new model (MT model) that describes the effect interparticle interactions on the superparamagnetic relaxation of *weakly interacting* particles and explains the observed behavior. Interestingly, there has been no further confirmation of the MT model by dc-magnetization / ac magnetic susceptibility measurements. All such studies have so far reported the opposite behavior: a decrease of T_B with decreasing interparticle interactions. As shown in Figure 3 (b), our dynamic susceptibility data demonstrates that both behaviors can in fact be present in the same system. T_B initially decreases with the decrease of the nanoparticle volume ratio for Φ within the $1/48 < \Phi < 1$ range, where the magnetic nanoparticles exhibit a transition

to a collective super-spin glass (SSG) state upon cooling in the presence of strong dipolar interactions. By further diluting the sample, however, T_B increases with decreasing Φ within a second regime, $1/384 < \Phi < 1/96$, where the weakly interacting superspins block individually upon cooling in a common superparamagnetic (SPM) transition.

The variation of T_B with the nanoparticle volume ratio Φ we have observed for diluted samples (weak dipolar interactions) is in agreement with the MT model prediction: a decrease of the relaxation times, thus an increase of the blocking temperature with the decrease of the dipolar interaction strength. This is clearly shown by the solid symbols in Fig. 4 that represent the measured T_B vs. Φ^2 dependence within the $1/384 < \Phi < 1/96$ range. To further confirm the microscopic origin of our observations we attempted linear fits to the T_B vs. Φ^2 data. The MT model predicts such a behavior. Indeed, if all parameters in Eq. (6) related to the Fe_3O_4 nanoparticle ensemble, i.e. the barrier to magnetization reversal KV, measurement time τ_m, average diameter D are fixed to Φ-independent values, the increase of T_B upon dilution is due to the dependence of ε on the nanoparticle volume ratio via $\varepsilon^{-6} = (\Phi/V)^2$ (see Eqn. (8) for reference); this yields a linear decrease of the blocking temperature with the square of the nanoparticle volume ratio. The solid line in Figure 4 shows such a linear fit within the $1/384 < \Phi < 1/96$ range. Although this analysis describes the increase of T_B with the decrease of interparticle interactions (predicted by the MT model), the fit has a rather large χ^2 residual. However, narrowing the Φ range to $1/384 < \Phi < 1/192$ (i.e. within weakest interparticle interaction regime) yields a linear fit (dashed line) with a much improved (by one order of magnitude) residual. This is particularly significant, as the MT model *is supposed* to provide a more accurate description of the system's magnetic behavior for very weak interactions.

3.3 Discussion of the Mørup-Tronc Model in Weakly Interacting Systems

The blocking temperatures used in the above analysis were determined from the peaks of the χ" vs. T curves collected at a given frequency of the driving field (10 kHz) for different values of Φ. For each of the four dilutions in the weak interaction regime we have also recorded the temperature dependence of the out of phase magnetic susceptibility at five frequencies. The χ" vs. T data collected at frequencies of 100 Hz, 1000 Hz, 3000 Hz, and 10000 Hz on the Φ = 1/384 sample are shown in Figure 5 (a); the solid lines are best fits to polynomial functions that allow a precise determination of the χ" peak temperature at each frequency. We collected similar data and performed similar analyses on the other three weakly interacting samples (nanoparticle volume ratios Φ = 1/96, 1/192, 1/240). We then used activation laws to fit the observed dependence of the blocking temperatures (T_B) on the frequency (f) / observation time (τ). These results are presented in Figure 5(b). The solid circles show the measured blocking temperatures at different observation times (T_B vs. τ) for the Φ = 1/384 sample, whereas the inverted triangles, filled squares, and upright triangles show the T_B vs. τ data for the Φ = 1/240, 1/192, and 1/96 samples, respectively. In all four cases, the solid lines are best fits of Eqn. 4, where *both* the interparticle-interaction-strength parameter, T_0, and the energy barrier to magnetization reversal E_B were allowed to vary as *independent* parameters. This approach is different from both the DBF model (where the energy barrier is varied but the interaction parameter is kept to $T_0 = 0$), and the SW model (where T_0 is varied but the barrier is kept fixed at $E_B = KV$). The values of the best fit parameters for the four samples are shown in the inset to Figure 5 (b). They indicate that T_0 decreases with the decrease of Φ (decrease of dipolar interparticle interactions) as expected, but the energy barrier E_B unexpectedly increases with the decrease of interparticle interactions.

This analysis shows that activation type laws provide an accurate quantitative description of the frequency dependence of the blocking behavior of weakly interacting Fe_3O_4 magnetic nanoparticle ensembles (volume ratios $1/384 < \Phi < 1/96$) if both T_o and E_B are allowed to vary as independent parameters. Yet, while the interaction strength parameter values yielded by the fits is consistent with the ensemble's dilution level, Φ, the energy barrier to magnetization reversal exhibits an unexpected dependence on Φ. On the other hand, the MT model accurately describes the observed T_B vs. Φ^2 behavior without any additional variable parameters. Moreover, the MT prediction only holds for weakly interacting nanoparticle ensembles, which is exactly where we observed the increase of the blocking temperature upon dilution. In conclusion, our data provides further experimental confirmation of the MT model validity, the first from ac-magnetic susceptibility measurements.

Chapter 4: Conclusions

We studied the superspin dynamics in 10 nm average size Fe_3O_4 magnetic nanoparticle ensembles. We found that the strength of the interparticle dipolar interactions (controlled by varying the nanoparticle volume ratio, Φ) has a strong effect on the system's blocking behavior. For strong interactions ($\Phi > 1/48$), the superparamagnetic ensemble undergoes a transition to a spin-glass-like state, i.e. the superspins freeze collectively upon cooling below a certain temperature threshold. This behavior is confirmed by fits to a dynamic scaling law known as a signature of spin glass freezing. In this regime, the temperature below which the superspins cease to rapidly reorient within the particle decreases as the nanoparticle volume ratio (interparticle interaction strength) is reduced. At low Φ values ($< 1/96$), i.e. for weak dipolar interactions, we observed a markedly different behavior: first, cooling each of these samples below a temperature T_B leads to the individual blocking of the superspins; second, an unexpected reentrant behavior of higher blocking temperatures occurs, where T_B increases back upon decreasing the nanoparticle volume ratio (and consequently the interparticle interaction strength).

Our analysis of ac-susceptibility in this weakly-interacting regime also reveals a surprising dependence of the energy barrier to magnetization reversal on the ensemble's dilution ratio. Decreasing the interaction parameter with decreasing Φ has led to the surprising observation of a dependence of the energy barrier on the ensemble's volume ratio. Additional work is needed to further elucidate the dynamic relationship between the energy barrier, interaction parameter, and Φ, however, it remains clear that a reentrant blocking behavior of T_B does occur above a particle concentration threshold. The T_B vs Φ^2 dependence within this weak-

interaction regime is very well described by the Mørup-Tronc (MT) model, making our results the first independent confirmation of this theory.

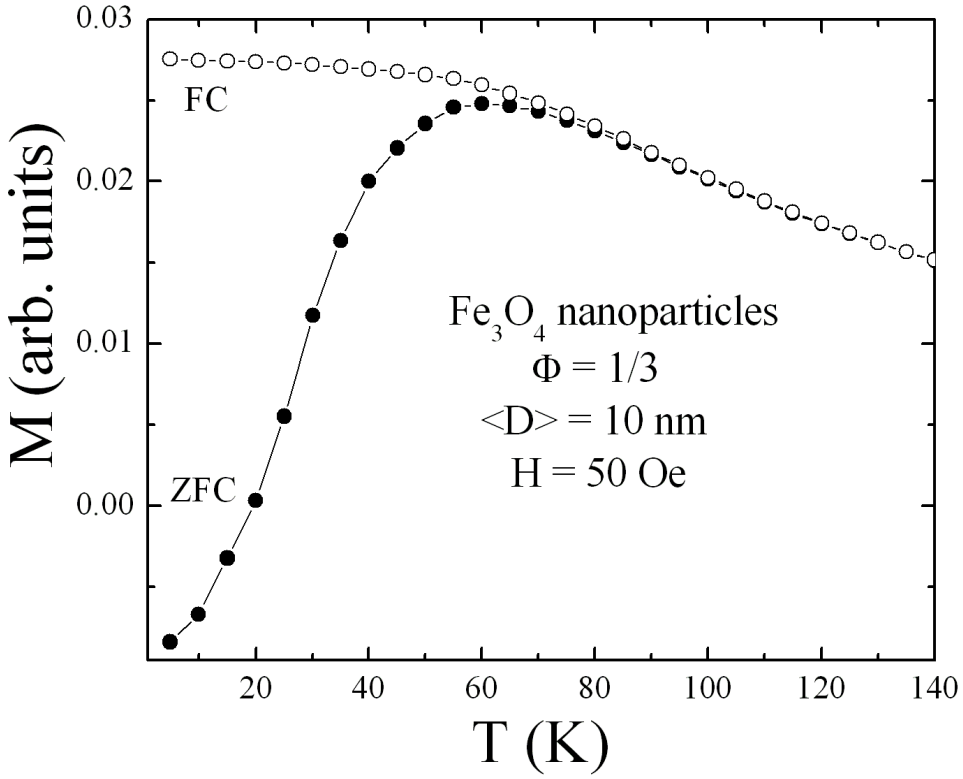

Figure 1 Temperature dependence of the dc-magnetization, M vs. T, collected upon heating an ensemble of Fe_3O_4 nanoparticles of volume ratio $\Phi = 1/3$ in an external magnetic field of 50 Oe using the field-cooled (FC) – zero field cooled (ZFC) protocol.

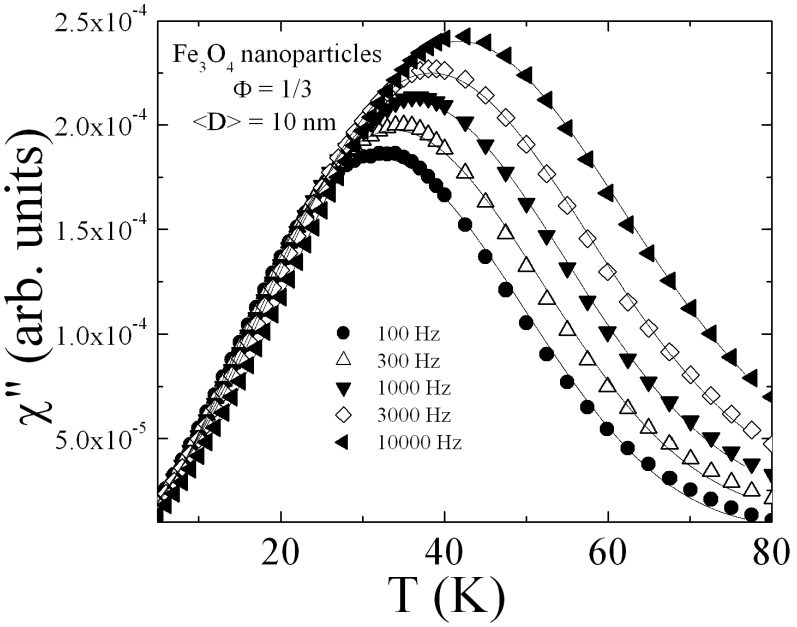

Figure 2 (a) Temperature dependence of the out of phase magnetic susceptibility χ" vs. T collected at five different frequencies 10 Hz, 100 Hz, 1000 Hz, 3000 Hz and 10000 Hz on a dense (Φ = 1/3) sample. The solid lines are best fits to polynomial functions that allow the susceptibility peak temperature to be determined for each measurement frequency.

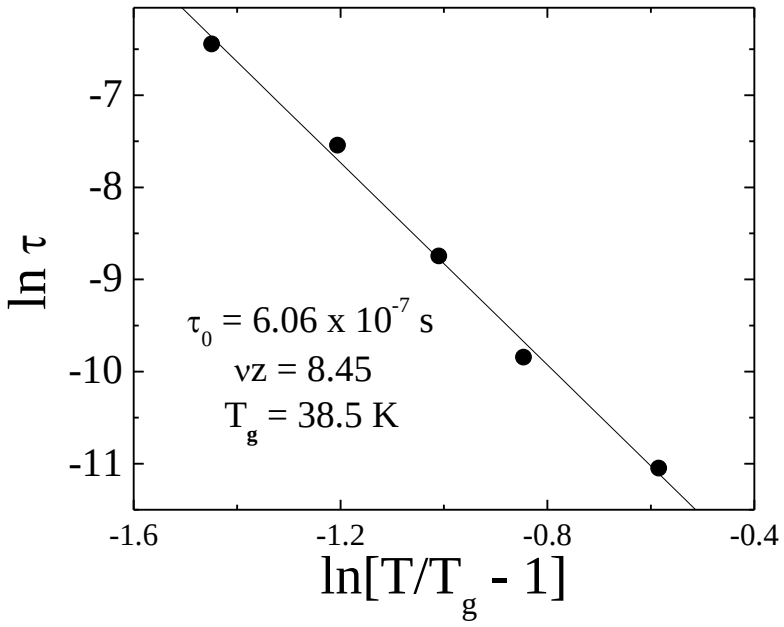

Figure 2 (b) Frequency / observation time dependence of the susceptibility peak on the reduced temperature (filled symbols) determined from the χ" vs. T data in Figure 2 (a). The solid line is a best fit of $\tau = \tau_o[(T/T_g)-1]^{-z\nu}$ to the data that allows the determination of the superspin freezing temperature T_g.

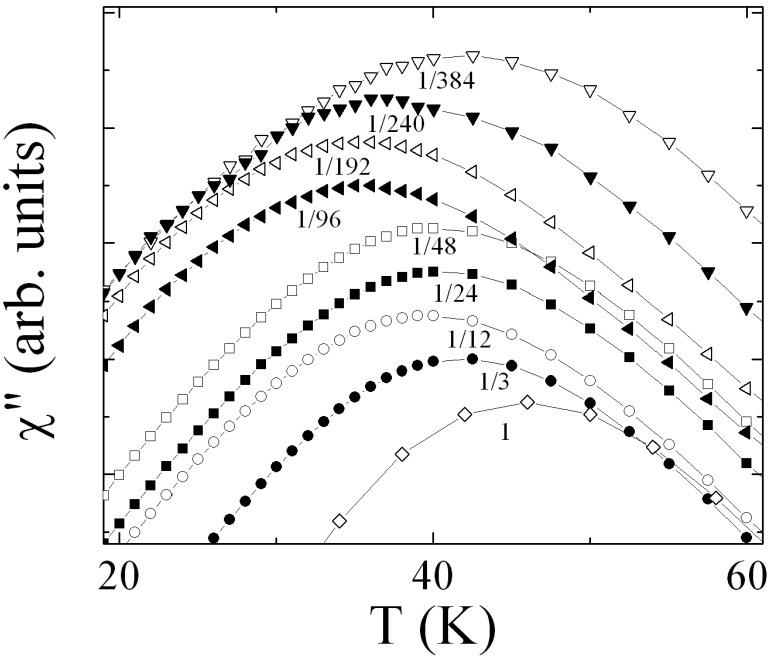

Figure 3 (a) Temperature dependence of the out-of-phase susceptibility χ" vs. T collected at a frequency f = 10000 Hz on Fe_3O_4 nanoparticle ensembles of different volume ratios: Φ = 1, 1/3, 1/12, 1/24, 1/48, 1/96, 1/192, 1/240, 1/384.

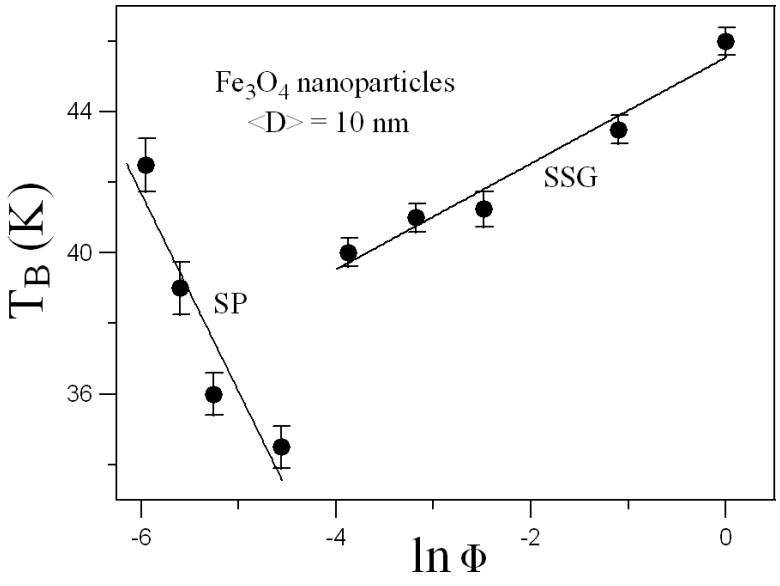

Figure 3 (b) Blocking / critical temperature T_B variation with the volume ratio Φ. In the strong interaction regime ($1/48 < \Phi < 1$) T_B decreases with the decrease of Φ; in the presence of weaker interactions ($1/96 < \Phi < 1/384$) the opposite behavior is observed, i.e. higher T_B values progressively reenter as Φ decreases.

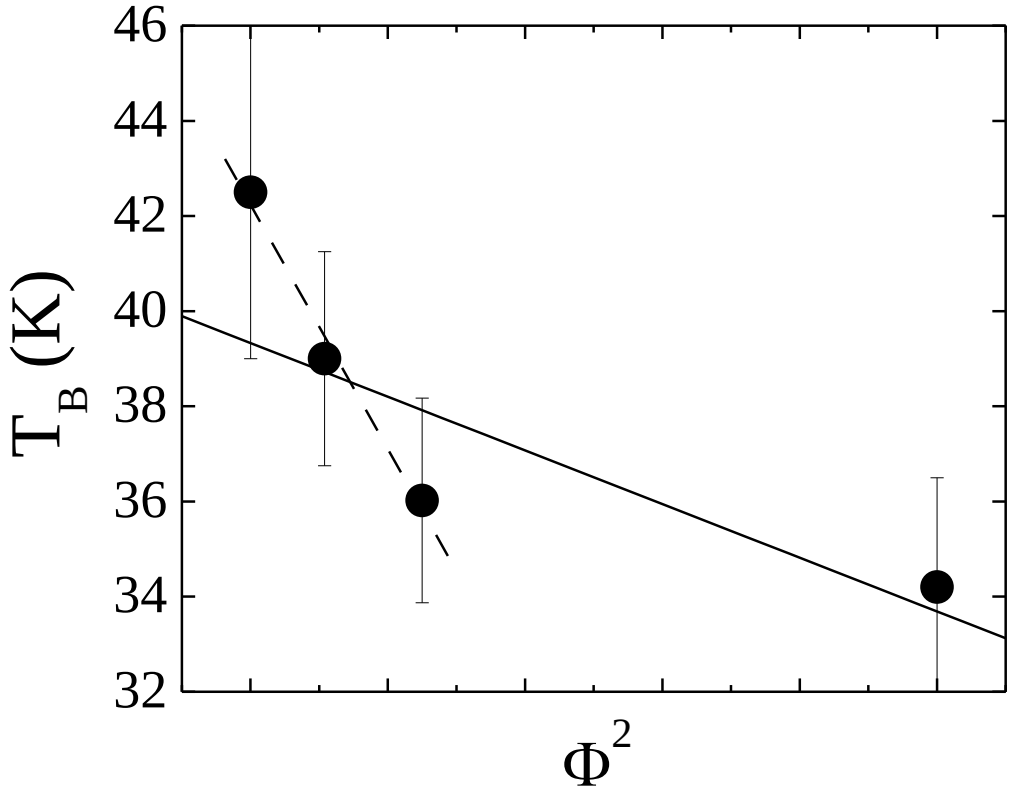

Figure 4 Observed blocking temperature dependence on the nanoparticle volume ratio: T_B vs. Φ^2 (solid symbols). The solid and dashed lines are linear fits to the Mørup-Tronc (MT) model within the ($1/96 < \Phi < 1/384$) and the ($1/192 < \Phi < 1/384$) range, respectively.

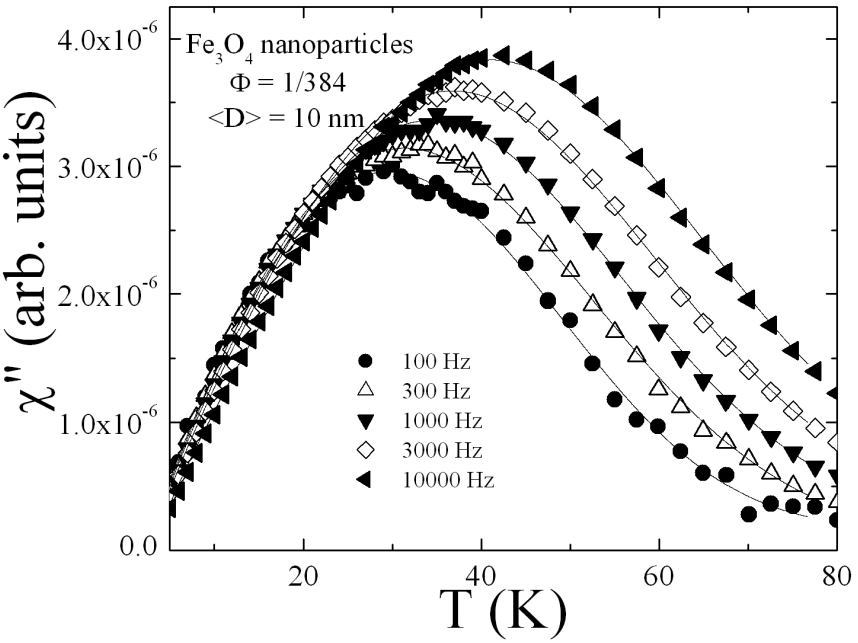

Figure 5 (a) Temperature dependence of the out of phase magnetic susceptibility χ" vs. T collected at five different frequencies 10 Hz, 100 Hz, 1000 Hz, 3000 Hz and 10000 Hz on a dilute (Φ = 1/384) sample . The solid lines are best fits to polynomial functions that allow the susceptibility peak temperature to be determined for each measurement frequency.

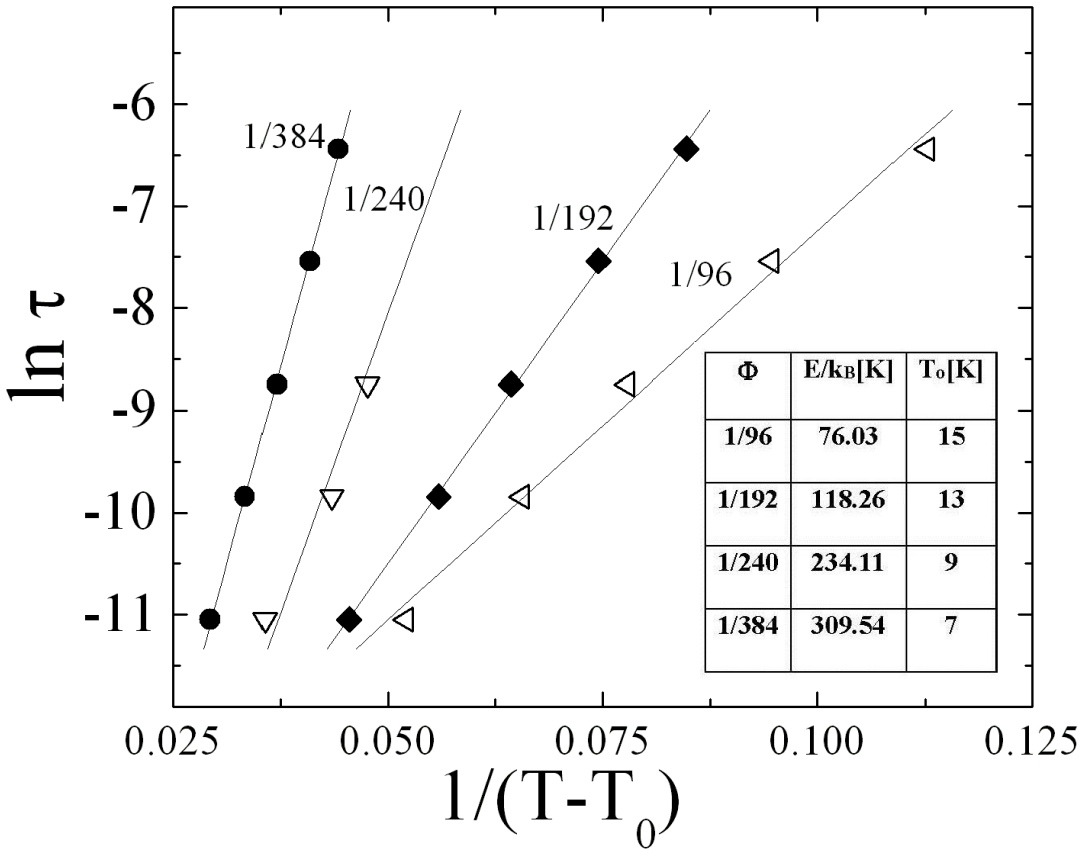

Φ	E/kB[K]	To[K]
1/96	76.03	15
1/192	118.26	13
1/240	234.11	9
1/384	309.54	7

Figure 5 (b) Frequency / observation time dependence of the susceptibility peak reduced temperature obtained from frequency-resolved ac-susceptibility data collected on weakly-interacting nanoparticle ensembles Φ = 1/96, 1/192, 1/240, 1/384.

References

[1] T. Nakamura, T. Miyamoto, and Y. Yamada, *J. Magn. Magn. Mater.* **256**, 340 (2003).

[2] R.D. Shull, *IEEE Trans. Mag.* **29**, 2614 (1993).

[3] Q.A. Pankhurst, J. Connolly, S.K. Jones, J. Dobson, *J. Phys. D: Appl. Phys.* **36**, R167 (2003).

[4] R. Hergt, S. Dutz, R. Muller, M. Zeisberger, *J. Phys.: Condens. Matter* **18**, S29219 (2006).

[5] P. Moroz. S.K. Jones, B.N. Gray, *Int. J. Hyperthermia* **18**, 267 (2002).

[6] J.L. Dormann, D. Fiorani, E. Tronc, *Adv. Chem. Phys.* **98**, 283 (1997).

[7] R.W. Chantrell, G.N. Coverdale, M. El Hilo, K.O'. Grady, *J. Magn. Magn. Mater.* **157**, 250 (1996).

[8] M. El Hilo, R.W. Chantrell, K.O' Grady, *J. Appl. Phys.* **84**, 5114 (1998).

[9] M.A. Zaluska-Kotur, *Phys. Rev. B* **54**, 1064 (1996).

[10] J.L. Dormann, L. Bessais, D. Fiorani, *J. Phys. C* **21**, 2015 (1988).

[11] J.O. Andersson, C. Djurgery, T. Jonsson, P. Svedlindh, P. Nordblad, *Phys. Rev. B* **56**, 13983 (1997).

[12] T. Jonsson, P. Svedlindh, M.F. Hansen, *Phys. Rev. Lett.* **81**, 3976 (1998).

[13] S. Mørup, *Hyperfine Inter.* **90**, 171 (1994).

[14] Neel L *Ann. Geophys*. **5** 99 (1949).

[15] Brown W F *Phys. Rev*. **130** 1677 (1963).

[16] Kodama R H, Berkowitz A E, McNiff E J Jr and Foner S *Phys. Rev. Lett.* **77** 394 (1996).

[17] Martinez B, Obradors X, Ballcels L I, Rouanet A and Monty C *Phys. Rev. Lett.* **80** 181 (1998).

[18] Sahoo S, Petracic O, Binek Ch, Kleenman W, Sousa J B, Cardoso S and Freitas P P *Phys. Rev. B* **65** 134406 (2002).

[19] Sahoo S, Petracic O, Kleenman W, Stappert S, Dumpich G, Nordblad P, Cardoso S and Freitas P P *Appl. Phys. Lett.* **82** 4116 (2003).

[20] G.F. Goya, T.S. Berquo, F.C. Fonseca, M.P. Morales *Journal of Applied Physics* **94**, 3520 (2003).

[21] L. Neel *Low Temp. Phys.* **413** (1962).

[22] X. Chen, S. Bendata, O. Petracic, W. Kleemann, S. Sahoo, S. Cardoso, P.P. Freitas *Phys. Rev. B* **72**, 214436 (2005).

[23] K. Binder, A.P. Young *Phys. Rev. B* **29**, 2864 (1984).

[24] C. Djurberg, P. Svedlindh, P. Nordblad, M.F. Hansen, F. Bodker, S. Mørup *Phys. Rev. Lett.* **79**, 5154 (1997).

[25] S. Shtrikman, E. P. Wohlfarth *Phys. Lett. A* **85**, 467 (1981).

[26] S. Mørup, E. Tronc *Phys. Rev. Lett*. **72**, 3278 (1994).

[27] P. Prene, E. Tronc, J.P. Jolivet, J. Livage, R. Cherkaoui, M. Nogues, J.L. Dormann, D. Fiorani *IEEE Trans. Magn.* **29**, 2658 (1993).

[28] T.N. Lan, T.H. Hai *Appl. Of Monte Carlo Method in Sci. and Engin.* 495 (2011).

[29] M. El-Hilo, K. O'Grady, R.W. Chantrell *J. Magn. Magn Mater.* **114**, 295 (1992).

[30] W. Luo, S.R. Rosenbaum, T.F. Rosenbaum, R.E. Rosensweig, *Phys. Rev. Lett.* **67**, 2721 (1991).

[31] S. Mørup, *Hyperfine Inter.* **60**, 959 (1990).

[32] S. Mørup, M.B. Madsen, J. Franck *J. Magn. Magn Mater.* **40**, 163 (1983).

[33] Le Bail A, Duroy H and Fourquet J L *Mater. Res. Bull*. 23 447 (1998).

[34] C.P. Bean *J. Appl. Phys.* **26**, 1381 (1955).

[35] R.J. Tackett, J.G. Parsons, B.I. Machado, S.M. Gaytan, L.E. Murr, C.E. Botez *Nanotech.* **21**, 365703 (2010).

[36] L. Neel *Ann. Geophys.* **5**, 99 (1949).

[37] R.H. Kodama, A.E. Berkowitz, E.J. McNiff Jr., S. Foner *Phys. Rev. Lett.* **77**, 394 (1996).

[38] S. Sahoo, O. Petracic, Ch. Binek, W. Kleenman, J.B. Sousa, S. Cardoso, P.P Freitas *Phys. Rev. B.* **65**, 134406 (2002).

[39] T. Jonsson, J. Mattsson, C. Djurberg, F. A. Khan, P. Nordblad, P. Svedlindh, *Phys. Rev. Lett.* **75**, 4138 (1995).

Vita

Joshua L. Morris is a life-long El Pasoan, born and raised on the slopes of the Franklin Mountains and under the desert sun. He graduate from Cathedral High School and enrolled at the University of Texas at El Paso where he has completed his Bachelor's and Master's in Physics. He worked with Dr. Cristian Botez in the Crystal Structure and Physical Properties Laboratory for the duration of his studies, publishing several papers in journals such as *Chemical Physics*. During the final year of his graduate coursework , Joshua had the honor of returning to Cathedral High School to teach an advanced physics course to help give his students the physics experience he wish he had received there.

His physics education has a wonderful and enlightening experience, opening his mind to new ways of thinking about the world and assessing problems and challenges. He is uncertain what the future holds, but with the solid foundation of a strong physical and mathematical education seasoned to perfection with meaningful research and professional experiences, he is confident (at least up to six-sigma) that he'll blaze his own trail towards personal success, and most importantly, happiness.

Joshua enjoys cooking, thinking up new recipes while he is running, and gardening (to grow his own ingredients to cook with) in his time away from the lab. When his mind isn't on food, he enjoys reading, coffee, and watching his way backwards through the best reviewed movies of every year with Allissa. The cats he and Allissa adopted are a constant source of joy and frustration for them; as Schrödinger and his cat wondered at the applicability of quantum uncertainty to the macroscopic world, Josh and Allissa wonder at the uncertainty of whether whatever the cats have knocked onto the floor this time has broken or not.

Permanent address: 652 Moondale Dr.
El Paso, TX, 79912-4236

This thesis/dissertation was typed by Joshua L. Morris.